Kinetic Study on the Reentrant Condensation of Oligonucleotide in Trivalent Salt Solution

Jihan Zhou, Fuyou Ke,* and Dehai Liang*

Beijing National Laboratory for Molecular Sciences and the Key Laboratory of Polymer Chemistry and Physics of Ministry of Education, College of Chemistry and Molecular Engineering, Peking University, Beijing, China, 100871

Received: August 6, 2010; Revised Manuscript Received: September 29, 2010

The reentrant condensation of 21-bp oligonucleotide in the presence of spermidine was investigated by laser light scattering and capillary electrophoresis. 21-bp oligonucleotide showed a bimodal distribution in 1×TE buffer, with the slow mode being the characteristic diffusion of polyelectrolyte in solution without enough salt. At the fixed spermidine concentration, the reentry of oligonucleotide underwent aggregation, phase separation, and disassociation in sequence with time, and the kinetics was extremely slow. For example, it took more than 1200 h (50 days) for the reentry to complete at 21 mM spermidine. Higher spermidine concentration led to faster kinetics. After reentry, the slow mode disappeared, and the charges of oligonucleotide were at least partially neutralized. No prominent charge inversion was observed. The kinetics of oligonucleotide reentry in the presence of spermidine gained insight in the interactions of polyelectrolyte in aqueous solution.

Introduction

DNA condensation has attracted a great deal of attention during the past 30 years mainly because of the importance for gene delivery and in understanding the biological process. There are many types of condensing agents,[1] including cationic liposomes and surfactants,[2−4] polycations,[5−7] multivalent salts,[8−10] organic solvents,[11−13] neutral flexible polymers,[14−16] and basic proteins.[1] Early studies indicate that trivalent salts or charged molecules of higher valence, such as biogenic polyamines, spermidine and spermine, are required to induce DNA to condense.[1] In aqueous solution, DNA condensation occurs when the degree of charge neutralization is more than 90%.[1] The driving force for DNA condensation is usually attributed to the like charge attraction originated from the correlation between counterions.[17]

Recently, a phenomenon called reentrant condensation has been widely investigated.[18] When an excess of multivalent salt is added to DNA solution, the condensed DNA is redissolved, and the extended conformation is recovered.[19] Besides DNA, polyelectrolyte with flexible chains, such as poly(styrenesulfonate),[20] shows similar behavior in the presence of multivalent counterions. Therefore, reentrant condensation is a common feature of polyelectrolytes.[21] However, traditional polyelectrolyte theories do not predict the redissolution of the condensed polyelectrolyte when the concentration of multivalent salt is high enough. Various mechanisms are proposed to explain the phenomenon. One theory suggested that the origin of redissolution was the screening of short-range attraction owing to high ionic strength in the solution.[20,21] Shklovskii and coworkers attributed the driving force to the charge inversion.[22,23] When an excess of multivalent salt is bound to DNA molecules, the net charge alters sign. The electrostatic repulsion dominates, resulting in chain expansion. The charge inversion in the presence of multivalent ions has been demonstrated by atomic force microscope, electrophoresis, and magnetic tweezers.[24,25] Wen and Tang reported that divalent counterions, such as Mg^{2+}, were not able to induce charge inversion on rodlike polyelectrolytes.[26] Solis and Olvera de la Cruz proposed a "two-state model",[27,28] suggesting that the charge inversion was not necessary because of the binding of co-ions and the screening of high ion strength. Moreover, they predicted that the charge inversion was closely correlated with the size of counterion, which was not included in Shklovskii's theory. The "two-state model" was further testified by experiments and simulations.[29−32] Hsiao reported that larger multivalent ions lead to a stronger degree of chain collapse and reexpansion, as well as a better charge neutralization.[31] Recently, Todd et al. suggested that the resolubilization of condensed DNA can be described by using the traditional Manning−Oosawa cation adsorption model, provided that cation−anion pairing at high electrolyte concentrations was taken into account.[33] Neither overcharging nor significant alterations in the condensed state are required to describe the resolubilization of condensed DNA.

Although the phase diagram based on DNA length, DNA concentration, multivalent salt concentration, and monovalent salt concentration has been constructed,[19,21,34] few studies on the behavior of oligonucleotide in the presence of multivalent salt have been conducted. Oligonucleotide is usually used as a model molecule because of its known chemical structure and monodispersity. The reentrant condensation of flexible or semiflexible chains involves both intra- and interchain interactions, which are responsible for collapse/reexpansion and aggregation/disassociation, respectively. However, double-stranded oligonucleotide within a certain length is considered as a rigid rod, and no chain collapse would occur during the condensation process, as predicted by the computer simulation.[35] It was also reported that the correlation of multivalent ions on the rod surface resulted in a strong attractive interaction.[36] With only aggregation/disassociation occurring with increasing multivalent counterions, oligonucleotide should offer a better approach to disclose the mechanism of reentrant condensation.

Herein we investigated the behavior of 21-bp oligonucleotide in aqueous solution with varying amount of spermidine by laser light scattering (LLS). Aggregation of oligonucleotides occurred with increasing spermidine concentration, and no disassociation

* Corresponding authors. Tel./Fax: +86-10-62756170 (D.L.). Tel.: 86-10-62767079 (F.K.). E-mail: dliang@pku.edu.cn (D.L.); kefew@pku.edu.cn (F.K.).

10.1021/jp1074187
Published on Web 10/11/2010

was observed even at 250 mM spermidine, a concentration much higher than that reported in the literature. Further study indicated that the reentry of oligonucleotides at fixed spermidine concentration was a kinetic process, which included three stages: aggregation, phase separation, and disassociation. The kinetics was closely related with the spermidine concentration.

Experimental Section

Material. Two complementary 21-nt oligonucleotides with random base sequence and >95% purity were purchased from SBS Genetech Co. Ltd. (Beijing, China). The double-stranded oligonucleotide was obtained by annealing the two complementary single chains at the same molar ratio in 1×TE buffer (10 mmol/L Tris, 1 mmol/L EDTA) at 95 °C for 5 min, followed by slow cooling to room temperature. The concentration of oligonucleotide was fixed at 0.05 mg/mL. Spermidine was purchased from Sigma-Aldrich (St. Louis, MO) and used as received. The stock solution (1.6 M) of spermidine was prepared by dissolving known amounts of sample in 1×TE buffer. Spermidine solutions at other concentrations were obtained by dilution in the same buffer. Poly(vinylpyrrolidone) (M = 30 kg/mol, CR) was purchased from Sinopharm Chemical Reagent Co. Ltd. (Beijing, China) and used as received. Milli-Q water (18.2 MΩ·cm) was used throughout the experiments.

LLS. A commercialized spectrometer from Brookhaven Instruments Corp. (BI-200SM goniometer, Holtsville, NY) was used to perform both static light scattering (SLS) and dynamic light scattering (DLS) over a scattering angular range of 15−155°. A vertically polarized, 100 mW solid-state laser (GXC-III, CNI, Changchun, China) operating at 532 nm was used as the light source, and a BI-TurboCo Digital Correlator (Brookhaven Instruments Corp.) was used to collect and process data. In static light scattering (SLS), the angular dependence of the excess absolute time-averaged scattered intensity, known as the Rayleigh ratio $R_{vv}(\theta)$, was measured. For a very dilute solution, the weight-averaged molar mass (M_w) and the root mean-square radius of gyration (R_g) can be obtained on the basis of

$$HC/R_{vv}(\theta) = (1/M_w)[1 + (1/3)R_g^2q^2] + 2A_2C \quad (1)$$

where $H = 4\pi^2n^2(dn/dC)^2/(N_A\lambda^4)$ and $q = 4\pi n/\lambda \sin(\theta/2)$ with N_A, n, dn/dC, and λ being Avogadro's number, the solvent refractive index, the specific refractive index increment, and the wavelength of light in a vacuum, respectively. In dynamic light scattering (DLS), the intensity−intensity time correlation function $G^{(2)}(\tau)$ in the self-beating mode was measured

$$G^{(2)}(\tau) = A[1 + \beta|g^{(1)}(\tau)|^2] \quad (2)$$

where A is the measured baseline, β is a coherence factor, τ is the delay time, and $g^{(1)}(\tau)$ is the normalized first-order electric field time correlation function. $g^{(1)}(\tau)$ is related to the line width distribution $G(\Gamma)$ by

$$g^{(1)}(\tau) = \int_0^\infty G(\Gamma)e^{-\Gamma\tau}\,d\Gamma \quad (3)$$

By using a Laplace inversion program, CONTIN,[37] the normalized distribution function of the characteristic line width $G(\Gamma)$ was obtained. The average line width, $\bar{\Gamma}$, was calculated according to $\bar{\Gamma} = \int\Gamma G(\Gamma)\,d\Gamma$. $\bar{\Gamma}$ is a function of both C and q, which can be expressed as

$$\bar{\Gamma}/q^2 = D(1 + k_dC)[1 + f(R_gq)^2] \quad (4)$$

with D, k_d, and f being the translational diffusive coefficient, the diffusion second virial coefficient, and a dimensionless constant, respectively. D can be further converted into the hydrodynamic radius R_h by using the Stokes−Einstein equation

$$D = k_BT/6\pi\eta R_h \quad (5)$$

where k_B, T, and η are the Boltzmann constant, the absolute temperature, and the viscosity of the solvent, respectively.

For LLS study, both spermidine and oligonucleotide solutions were filtered through a 0.22 μm PVDF membrane (Millipore, USA) to remove the dust. Known amounts of spermidine were added in the oligonucleotide, and the mixture was slightly shaken, and then stayed at room temperature for at least half an hour before the LLS measurements. For kinetic study, spermidine and oligonucleotide were mixed instantly, and the starting time was set as the point of mixing.

Capillary Electrophoresis (CE). CE was performed on a P/ACE MDQ system (Beckman Instruments, USA) with UV detection at 254 nm. A 40.2 cm (effective length: 30 cm) bare fused-silica capillary (Xinnuo Corp., Hebei, China) with 100 μm i.d. was used as the column. The capillary was pretreated sequentially by 1 N HCl for 10 min, 1×TE for 5 min, and an electric field of 300 V/cm for 10 min. 0.1% polyvinylpyrrolidone in 1×TE buffer was able to effectively suppress the electroosmosis flow, and was chosen as the running buffer.[38] Oligonucleotide with or without spermidine was injected at 0.5 psi for 3 s in the cathode end and pushed to the middle of the capillary. An electric field (the polarity was normal) of 200 V/cm was applied for 5 min. The sample was then pushed through the detector at 0.5 psi. With known flow rate of the buffer solution at 0.5 psi, the mobility of oligonucleotide was obtained.

Results and Discussion

Adding Spermidine into 21-bp Oligonucleotide. As reported in the literature,[19,21] condensed DNA is redissolved when the spermidine concentration is more than 100 mM, and it is independent of DNA concentration. In our study, the initial concentration of 21-bp oligonucleotide is fixed at 0.05 mg/mL, which is low enough to avoid precipitation and easier to be monitored by laser light scattering. First, we add spermidine into the oligonucleotide solution at the rate of one addition every half an hour. To avoid prominent changes in oligonucleotide concentration during titration, we use spermidine at much higher concentration than that of oligonucleotide. Figure 1 shows the excess scattered intensity at 30° with increasing spermidine concentration. When the concentration of spermidine is lower than 1 mM, the excess scattered intensity is almost constant, indicating no occurrence of aggregation. With further addition of spermidine, the intensity exponentially increases, suggesting the occurrence of heavy aggregation. The intensity reaches a maximum at 100 mM spermidine and starts to decline. However, after addition of 260 mM spermidine, the scattered intensity is still much stronger (at least 20×) than that before titration.

Figure 2 shows the hydrodynamic radius distribution of oligonucleotide at various amount of spermidine. Twenty-one bp oligonucleotide in 1×TE buffer without added spermidine

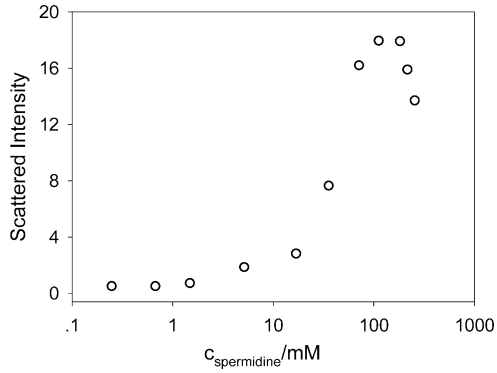

Figure 1. Changes in the excess scattered intensity at 30° with the addition of spermidine. Initial DNA concentration: 0.05 mg/mL. Initial spermidine concentration: 100 mM when the mixed concentration is <10 mM, and 1.6 M otherwise.

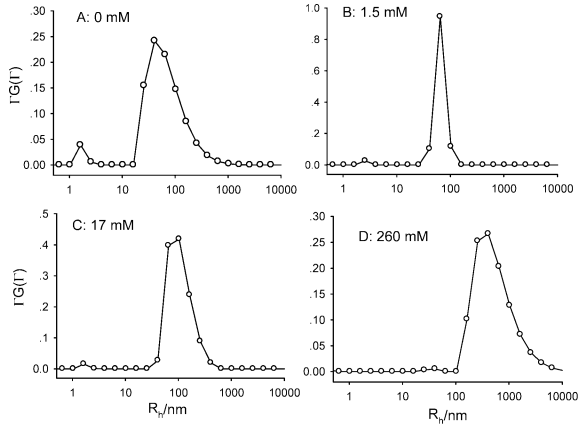

Figure 2. Hydrodynamic radius distribution at 30° at various concentrations of spermidine.

exhibits two relaxation modes (Figure 2A): a fast mode with $R_{h,app}$ about 1.6 nm, and a slow mode with $R_{h,app}$ about 50 nm. Since the slow mode is suppressed with the addition of enough amount of NaCl (Figure S1 in the Supporting Information), we attribute the phenomenon of oligonucleotide to the extraordinary behavior of polyelectrolyte in the regime where the added salt is not strong enough to screen the interchain interactions.[39] This phenomenon has been well reported in the literature.[40−42] It is commonly believed that the fast mode is due to the coupled diffusion of polyion with counterions, while the interpretation of the slow mode has not reached an agreement.[43−46] When spermidine is added to oligonucleotide to induce aggregation, the fast mode gradually disappears, while the size of the slow mode increases and its distribution narrows down (Figure 2B). After 1.5 mM, the distribution of the slow mode gradually broadens with further addition of spermidine (Figure 2C,D). Figure 3 shows changes in the apparent radius of gyration $R_{g,app}$ and the hydrodynamic radius $R_{h,app}$ (after extrapolation to zero angle) of the aggregates (or slow mode) during the titration process. Clearly, both $R_{g,app}$ and $R_{h,app}$ increase with increasing spermidine concentration. At spermidine concentration larger than 100 mM, in which region the excess scattered intensity decreases (Figure 1), the increase in both sizes is more drastic, and $R_{g,app}$ increases faster than $R_{h,app}$. The decrease in intensity and the increase in size suggest that the chain density of the aggregates becomes loose with increasing spermidine concentration.[47]

Kinetics of Reentrant Condensation. The decrease in the excess scattered intensity and the increase in the apparent size after addition of 100 mM spermidine imply the redissolvation

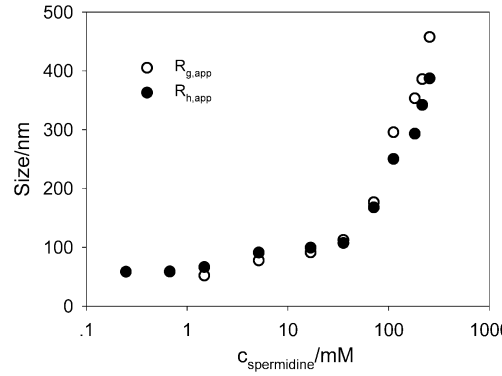

Figure 3. Spermidine concentration dependence of $R_{g,app}$ and $R_{h,app}$. The other conditions are the same as in Figure 1.

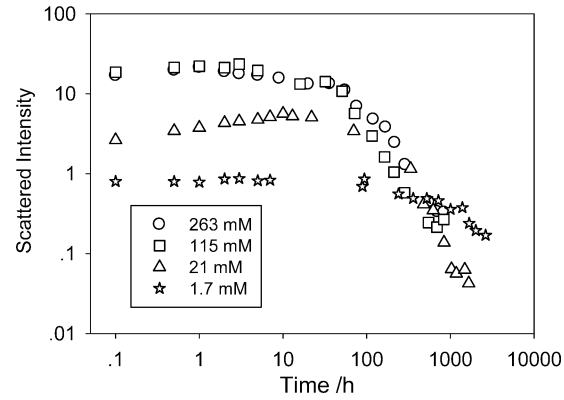

Figure 4. Change of light scattering intensity at 30° with time at different concentrations of spermidine. Initial DNA concentration 0.05 mg/mL.

of aggregates. The single oligonucleotides not being observed during the titration process is probably due to the slow kinetics of reentry. To test this hypothesis, we mixed known amounts of spermidine with oligonucleotide instantly, and then started to monitor the evolutional changes by LLS. On the basis of the phase diagram of DNA and spermidine in the literature,[19,21] we selected four different spermidine concentrations, 263, 115, 21, and 1.7 mM, while keeping the oligonucleotide concentration constant at 0.05 mg/mL. Figure 4 shows the time dependence of the scattered intensity measured at 30°. Similar results are obtained at other scattering angles. At the studied spermidine concentrations, all the scattered intensity curves show similar shapes: a slow increase, followed by a drastic drop at certain time point. The onset point of intensity drop is strongly dependent on the spermidine concentration, with higher concentration leading to earlier drop of scattered intensity. For example, the intensity starts to decrease after 10 h in the presence of 21 mM spermidine, whereas it only takes 1 h when the spermidine concentration increases to 263 mM. Eventually, the scattered intensity reaches a value much lower than that of the pure olignucleotide solution before mixing, but very close to that of the solvent. Note that the time period for the intensity to reach this level is also closely related with the spermidine concentration.

Figure 5 shows the time dependence of the hydrodynamic radius distribution of 21-bp oligonucleotides at 21 mM spermidine. Right after the mixing (5 min), only one diffusive mode, with $R_{h,app}$ about 87 nm, is observed in the system (Figure 5A).The size of the aggregate increases with time. After 10 h, the distribution becomes broad at the time point when the scattered intensity starts to decrease (Figure 5B). After about 330 h, the scattered intensity starts to fluctuate with extremely

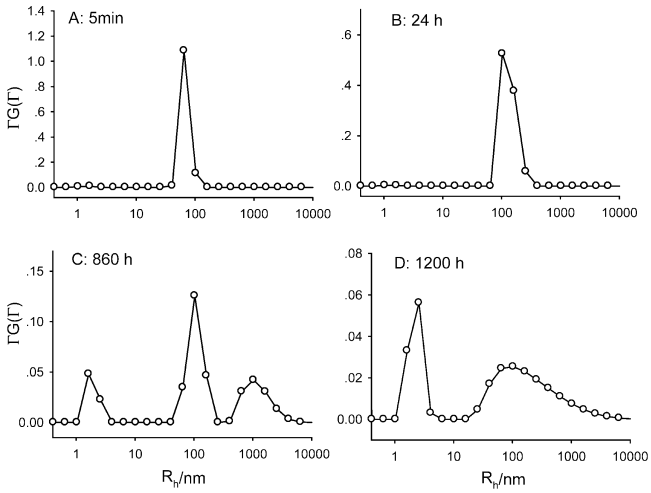

Figure 5. Time dependence of the hydrodynamic radius distribution of 21-bp oligonucleotides at 30°. Spermidine concentration: 21 mM.

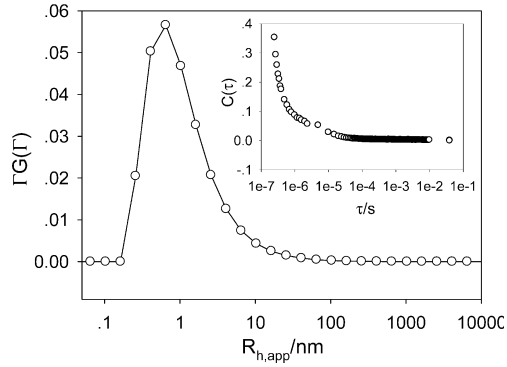

Figure 6. Size distribution of 21-bp oligonucleotides after reentry in the presence of 21 mM spermidine. The inset shows the corresponding correlation curve.

large amplitude, suggesting the formation of huge particles or phase separation. No valid correlation curve is able to be collected under such situations. The amplitude of fluctuation gradually decreases with time. At about 860 h, a trimodal distribution is detected from DLS (Figure 5C). Besides the primary aggregate, individual oligonucleotides and aggregates with the size about a micrometer are also observed. The micrometer-size aggregate is responsible for the heavy fluctuation of the scattered intensity. At this time period, both of the aggregates are slowly disassociating into single oligonucleotides, and the larger aggregates disassociates faster. Compared with that in Figure 5C, the area ratio of the oligonucleotide in Figure 5D increases with time at the cost of the other two. Since the scattered intensity is roughly proportional to the sixth power of particle size, the amount of large aggregates is much less than that of individual oligonucleotide. This also explains the decrease in scattered intensity in the presence of the aggregate with diameter in micrometers. Figure 6 shows the COTIN results and the corresponding correlation curve at 30° after 1200 h. Clearly, only single oligonucleotide remains in the system. Note that the $R_{h,app}$ of the oligonucleotide in Figure 6 is about 0.7 nm, smaller than the size (1.6 nm) determined from the sample before titration (Figure 2A). This is due to the salt, whose contribution to the total scatted intensity sharply increases as the aggregates disappears.[48]

Similar results are observed at other spermidine concentrations. Figure 7 compares the evolutional size change of the aggregates at 21 and 263 mM spermidine. Clearly, the $R_{g,app}$ and $R_{h,app}$ of aggregates formed at 263 mM spermidine are much larger and increase faster than those of aggregates formed at 21 mM spermidine. And the heavy fluctuation of scattered intensity also occurs (where no data point is shown) earlier at 263 mM spermidine. Combining Figures 4 and 7 together, we can see that the sizes keep increasing at the time period when the scattered intensity has been declining. For example, in the presence of 21 mM spermidine, the scattered intensity starts to decrease at 10 h (Figure 4), while the size keeps increasing for 330 h (Figure 7). This suggests that the formed particles become loose in chain density after 10 h.

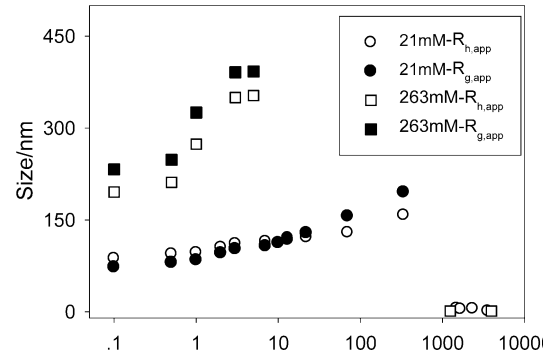

Figure 7. Time dependence of $R_{g,app}$ and $R_{h,app}$ of the aggregates in the presence of 21 and 263 mM spermidine.

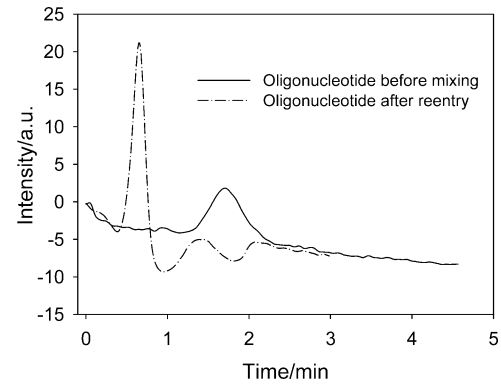

Figure 8. Electropherograms of oligonucleotide with and without 115 mM spermidine. The details are described in the Experimental Section.

Effective Charge on Oligonucleotide after Reentry. In the presence of spermidine, 21-bp oligonucleotide undergoes a complicated reentry process with time, and eventually stays as single chains. Since spermidine is positively charged, opposite to oligonucleotide, it is crucial to determine the effective charge on oligonucleotide after reentry. The size of 21-bp oligonucleotide is small, and conventional ζ-potential analyzer does not yield valid results. Therefore, we conducted capillary electrophoresis experiment to determine the mobility of oligonucleotide before and after reentry. Since the reentry process of oligonucleotide is similar at different spermidine concentrations, we only studied the oligonucleotide in the presence of 115 mM spermidine by capillary electrophoresis. Figure 8 shows the electropherogram of oligonucleotide under different conditions. On the basis of the migration time, the mobility of oligonucleotide without spermidine is determined to be 3.5×10^{-4} cm^2 V^{-1} s^{-1}, close to the values reported in literature.[49,50] The mobility is calculated to $(0.0 \pm 0.3) \times 10^{-4}$ cm^2 V^{-1} s^{-1} in the presence of 115 mM spermidine, suggesting that the binding of spermidine on the oligonucleotide occurs during the reentry process. The near zero value also indicates that the charge inversion is not prominent.

Reentry Controlled by Kinetics. The reentrant condensation of oligonucleotide is quite different from that of longer DNA chains, where the kinetics of redissolution is transient, and only aggregates form (no reentry) at spermidine concentration below 100 mM.[19] We attribute the unusual reentrant condensation of oligonucleotide in the presence of spermidine to the chain conformation of oligonucleotide. Twenty-one bp oligonucleotide exhibits a bimodal distribution: single chains coexist with the slow mode (Figure 2A). The slow mode could be attributed to temporal aggregates or multimacroion domains.[46,51] After reentrant condensation in the presence of spermidine, the slow mode disappears, and 21-bp oligonucleotide stays as single chains with charges at least partially neutralized. Our time-resolved LLS results clearly reveal that this transition (reentrant condensation) undergoes three stages: aggregation (or complexation), phase separation, and disassociation. In the aggregation process, the spermidine-induced attraction between oligonucleotides results in the formation of large aggregates. Since the slow mode of oligonucleotide is larger in size and contains more chains, it serves as the precursor of aggregates (precisely, spermidine/oligonucleotide complex) (Figures 2 and 5). In other words, the growth of the aggregate is based on the slow mode instead of single oligonucleotide, which agrees with our previous findings in other complex system.[52] The size of the aggregate increases with time. After a certain time, the chain density becomes loose as demonstrated by the decrease in the scattered intensity. This also suggests that the major driving force for aggregation is not hydrophobic attraction derived from charge neutralization, but mainly the short-range electrostatic attractions caused by counterion condensation on polymer chains. Different models, such as the "ion-bridging" model developed by Olvera de la Cruz et al.,[53] have been proposed to describe this attraction forces. In this model, the alternation of the negative and positive charges along the polymer chain is random, while in the model developed by Rouzina and Bloomfield, the alternation of the charges is periodic.[54] In both models, the attraction force is dependent on the effective charge of polyelectrolyte.

Phase separation, as indicated by the heavy intensity fluctuation, occurs when the size of aggregates reaches a certain value. Even though we do not obtain a valid correlation curve during phase separation, we can deduce from Figure 5C that large amount of micrometer-size clusters form in the system. The length of oligonucleotide is short, and the condensation of the spermidine on the chain could be dynamic. Since the electrostatic attraction is weakened due to the screening by an excess of multivalent counterions,[21] the neutralization of oligonucleotide by spermidine results in weak binding of the formed aggregates or clusters. The kinetics of charge neutralization is controlled by both the diffusion rate of spermidine to each oligonucleotide, and the rate of binding to oligonucleotide. The slow mode of oligonucleotide certainly hinders the neutralization process, leading to a slow kinetics. When the charge on the oligonucleotide is neutralized to a certain value, the aggregates are unstable and disassociation occurs. This disassociation process is extremely slow and dependent on the spermidine concentration; e.g., in the presence of 263 mM spermidine, it takes 3 h to phase separate, but more than 600 h for the disassociation to complete. After reentry, 21-bp oligonucleotide stays as single chains with charges at least partially neutralized. Since prominent charge inversion is not observed, the transition of aggregates to single chain results from the screening of the short-range electrostatic attractions and the translational entropy of the chains.[21,55]

Conclusions

Using 21-bp oligonucleotide as an example, we studied the kinetics of the reentrant condensation of short, rodlike polyelectrolyte in the presence of multivalent salts. Even though without chain condensation or relaxation, the reentry of oligonucleotide underwent aggregation, phase separation, and disassociation in sequence with time, and the kinetics was extremely slow especially when the spermidine concentration was not high enough. The disappearance of the slow mode (temporal aggregates of oligonucleotides) after reentry suggested that chain conformation also played a key role on the kinetics of reentrant condensation. Our work further revealed the interaction mechanism of polyelectrolyte with multivalent counterions.

Acknowledgment. Financial support of this work from the National Natural Science Foundation of China (20774004, 20990232) is gratefully acknowledged.

Supporting Information Available: Figure showing effect of NaCl concentration on the size distribution of oligonucleotide. This material is available free of charge via the Internet at http://pubs.acs.org.

References and Notes

(1) Bloomfield, V. A. *Curr. Opin. Struct. Biol* **1996**, *6* (3), 334–341.
(2) Mahato, R. I.; Rolland, A.; Tomlinson, E. *Pharm. Res.* **1997**, *14* (7), 853–859.
(3) Le Ny, A. L. M.; Lee, C. T. *J. Am. Chem. Soc.* **2006**, *128*, 6400–6408.
(4) Marchetti, S.; Onori, G.; Cametti, C. *J. Phys. Chem. B* **2005**, *109*, 3676–3680.
(5) Pouton, C. W.; Lucas, P.; Thomas, B. J.; Uduehi, A. N.; Milroy, D. A.; Moss, S. H. *J. Controlled Release* **1998**, *53* (1−3), 289–299.
(6) De Smedt, S. C.; Demeester, J.; Hennink, W. E. *Pharm. Res.* **2000**, *17* (2), 113–126.
(7) Kunath, K.; von Harpe, A.; Fischer, D.; Peterson, H.; Bickel, U.; Voigt, K.; Kissel, T. *J. Controlled Release* **2003**, *89* (1), 113–125.
(8) Bloomfield, V. A. *Biopolymers* **1991**, *31* (13), 1471–1481.
(9) Bloomfield, V. A. *Biopolymers* **1997**, *44* (3), 269–282.
(10) Vijayanathan, V.; Thomas, T.; Shirahata, A.; Thomas, T. J. *Biochemistry* **2001**, *40*, 13644–13651.
(11) Arscott, P. G.; Ma, C. L.; Wenner, J. R.; Bloomfield, V. A. *Biopolymers* **1995**, *36* (3), 345–364.
(12) Mel'nikov, S. M.; Khan, M. O.; Lindman, B.; Jonsson, B. *J. Am. Chem. Soc.* **1999**, *121*, 1130–1136.
(13) Roy, K. B.; Antony, T.; Sakena, A.; Bohidar, H. B. *J. Phys. Chem. B* **1999**, *103*, 5117–5121.
(14) Lerman, L. S. *Proc. Natl. Acad. Sci. U.S.A.* **1971**, *68* (8), 1886–1890.
(15) Pastre, D.; Hamon, L.; Mechulam, A.; Sorel, I.; Baconnais, S.; Curmi, P. A.; Le Cam, E.; Pietrement, O. *Biomacromolecules* **2007**, *8*, 3712–3717.
(16) Ramos, J. E. B.; de Vries, R.; Neto, J. R. *J. Phys. Chem. B* **2005**, *109*, 23661–23665.
(17) Ha, B. Y.; Liu, A. J. *Phys. Rev. Lett.* **1997**, *79* (7), 1289–1292.
(18) Nguyen, T. T.; Rouzina, I.; Shklovskii, B. I. *J. Chem. Phys.* **2000**, *112* (5), 2562–2568.
(19) Pelta, J.; Livolant, F.; Sikorav, J. L. *J. Biol. Chem.* **1996**, *271* (10), 5656–5662.
(20) Delacruz, M. O.; Belloni, L.; Delsanti, M.; Dalbiez, J. P.; Spalla, O.; Drifford, M. *J. Chem. Phys.* **1995**, *103* (13), 5781–5791.
(21) Raspaud, E.; de la Cruz, M. O.; Sikorav, J. L.; Livolant, F. *Biophys. J.* **1998**, *74* (1), 381–393.
(22) Shklovskii, B. I. *Phys. Rev. E* **1999**, *60* (5), 5802–5811.
(23) Grosberg, A. Y.; Nguyen, T. T.; Shklovskii, B. I. *Rev. Mod. Phys.* **2002**, *74* (2), 329–345.
(24) Besteman, K.; Zevenbergen, M. A. G.; Heering, H. A.; Lemay, S. G. *Phys. Rev. Lett.* **2004**, *93* (17), 170802.
(25) Besteman, K.; Van Eijk, K.; Lemay, S. G. *Nat. Phys.* **2007**, *3* (9), 641–644.
(26) Wen, Q.; Tang, J. X. *J. Chem. Phys.* **2004**, *121* (24), 12666–12670.
(27) Solis, F. J.; de la Cruz, M. O. *J. Chem. Phys.* **2000**, *112* (4), 2030–2035.
(28) Solis, F. J. *J. Chem. Phys.* **2002**, *117* (19), 9009–9015.
(29) Jan, J. S.; Breedveld, V. *Macromolecules* **2008**, *41*, 6517–6522.

(30) Hsiao, P. Y.; Luijten, E. *Phys. Rev. Lett.* **2006**, *97* (14), 148301.
(31) Hsiao, P. Y. *J. Phys. Chem. B* **2008**, *112*, 7347–7350.
(32) May, S.; Iglic, A.; Rescic, J.; Maset, S.; Bohinc, K. *J. Phys. Chem. B* **2008**, *112*, 1685–1692.
(33) Todd, B. A.; Rau, D. C. *Nucleic Acids. Res.* **2008**, *36* (2), 501–510.
(34) Chien, F. T.; Lin, S. G.; Lai, P. Y.; Chan, C. K. *Phys. Rev. E* **2007**, *75* (4), 041922.
(35) Wei, Y. F.; Hsiao, P. Y. *J. Chem. Phys.* **2007**, *127* (6).
(36) GronbechJensen, N.; Mashl, R. J.; Bruinsma, R. F.; Gelbart, W. M. *Phys. Rev. Lett.* **1997**, *78* (12), 2477–2480.
(37) Provencher, S. W. *Comput. Phys. Commun.* **1982**, *27*, 229–242.
(38) Gao, Q. F.; Yeung, E. S. *Anal. Chem.* **1998**, *70*, 1382–1388.
(39) Forster, S.; Schmidt, M. *Adv. Polym. Sci.* **1995**, *120*, 51–133.
(40) Sedlak, M. *J. Chem. Phys.* **1996**, *105* (22), 10123–10133.
(41) Ermi, B. D.; Amis, E. J. *Macromolecules* **1998**, *31*, 7378–7384.
(42) Zhou, K. J.; Li, J. F.; Lu, Y. J.; Zhang, G. Z.; Xie, Z. W.; Wu, C. *Macromolecules* **2009**, *42*, 7146–7154.
(43) Sedlak, M. *Macromolecules* **1995**, *28*, 793–794.
(44) Borsali, R.; Nguyen, H.; Pecora, R. *Macromolecules* **1998**, *31*, 1548–1555.
(45) Skibinska, L.; Gapinski, J.; Liu, H.; Patkowski, A.; Fischer, E. W.; Pecora, R. *J. Chem. Phys.* **1999**, *110* (3), 1794–1800.
(46) Schmitz, K. S. *J. Phys. Chem. B* **2009**, *113*, 2624–2638.
(47) Burchard, W. *Adv. Polym. Sci.* **1983**, *48*, 1–124.
(48) Sedlak, M. *Langmuir* **1999**, *15*, 4045–4051.
(49) Bunz, A. P.; Barron, A. E.; Prausnitz, J. M.; Blanch, H. W. *Ind. Eng. Chem. Res.* **1996**, *35*, 2900–2908.
(50) Hammond, R. W.; Oana, H.; Schwinefus, J. J.; Bonadio, J.; Levy, R. J.; Morris, M. D. *Anal. Chem.* **1997**, *69*, 1192–1196.
(51) Sedlak, M. *Macromolecules* **1993**, *26*, 1158–1162.
(52) Deng, L.; Wang, C. H.; Li, Z. C.; Liang, D. H. *Macromolecules* **2010**, *43*, 3004–3010.
(53) Olvera de la Cruz, M.; Belloni, L.; Delsanti, M.; Dalbiez, J. P.; Spalla, O.; Drifford, M. *J. Chem. Phys.* **1995**, *103* (13), 5781–5791.
(54) Rouzina, I.; Bloomfield, V. A. *J. Phys. Chem.* **1996**, *100*, 9977–9989.
(55) Toma, A. C.; de Frutos, M.; Livolant, F.; Raspaud, E. *Biomacromolecules* **2009**, *10*, 2129–2134.

JP1074187